Auger electron spectroscopy analysis of chromium depletion in a model Ni-16Cr-9Fe alloy oxidized at 950°C

André Nicolas, Vincent Barnier, Edwige Aublant, Krzysztof Wolski

Auger electron spectroscopy analysis of chromium depletion in a model Ni–16Cr–9Fe alloy oxidized at 950 °C

André Nicolas,[a,b,c] Vincent Barnier,[c] Edwige Aublant[a] and Krzysztof Wolski[c,*]

[a]*AREVA NP, Centre Technique, Département Corrosion-Chimie, 30 Bd de l'Industrie, 71200 Le Creusot, France*
[b]*ENISE, UMR 5513, LTDS, Université de Lyon, 54 Rue Jean Parot, 42023 Saint Etienne, France*
[c]*Ecole des Mines de Saint-Etienne, Laboratoire Claude Goux UMR CNRS 5146, Centre SMS, 158 Cours Fauriel, 42023 Saint Etienne, France*

A complete chromium depletion profile with its depth resolution in the nanometre range was obtained on a Ni–16Cr–9Fe model alloy after a 10 h oxidation at 950 °C in air. Auger electron spectroscopy coupled to ion sputtering and energy-dispersive X-ray spectroscopy were used to measure the chromium depletion profile. The chromium content at the oxide/alloy interface is below 0.5 wt.%. This exceptionally low Cr content is in agreement with Wagner's model for binary alloys.

Keywords: Oxidation; Auger electron spectroscopy (AES); Nickel alloys; Interface diffusion; Chromium depletion

High-temperature oxidation of industrially relevant alloys, containing typically between 16 and 30 wt.% Cr, results in the formation of a protective chromium-rich oxide scale. One of the major types of damage induced in the substrate by the growth of chromium-rich oxides is chromium depletion, which was theoretically assessed by Wagner [1]. This depletion is known to be high in all face-centred cubic (fcc) alloys [2,3] due to the relatively low Cr diffusion coefficient. Mechanisms of such depletion have been extensively studied in the 800–1000 °C temperature range using model binary Ni–Cr alloys [4–9] and energy-dispersive X-ray spectrometry (EDX) on polished cross-sections at a micrometre scale. These results have allowed experimental Cr depletion profiles to be established and the chromium diffusion coefficient to consequently be determined. The Cr concentration at the oxide/alloy interface has been shown to be frequently close to half of the bulk Cr content of the alloy and never lower than 5 wt.%. Attempts to extrapolate a Cr concentration profile between the area of EDX validity and the exact oxide/alloy interface position have also resulted in an interfacial chromium concentration in the range of 10 wt.% [10]. Consequently, the spatial resolution of EDX performed on polished cross-sections appears to be a limitation, and the real chromium content close to the oxide/alloy interface cannot be assessed by this widely used spectrometry, in particular in the range between 0 and 1.5 μm for a typical 15 keV accelerating voltage.

In this paper, we report a complete chromium depletion profile obtained in a Ni–16Cr–9Fe model alloy after a 10 h oxidation at 950 °C in air with special emphasis on the first tens/hundreds of nanometres beneath the oxide/alloy interface, as analysed by auger electron spectroscopy (AES) coupled with ion sputtering. We discuss this result in the frame of a classical Wagner's analytical solution for binary alloys [1].

Experiments were performed on cylindrical platelets ($\varphi = 18$ mm, $h = 2$ mm) of Ni–16Cr–9Fe model alloy with impurity concentrations lower than 10 ppm (LECO analysis of C, S, O and N). Sample surfaces were mechanically polished using SiC papers down to grade 1200 and diamond paste down to 0.25 μm. No chemical attack was performed.

High-temperature oxidations were performed at 950 °C for either 10 or 100 h. Three different oxidation procedures were used (Table 1): first, an oxidation in a standard furnace with a very slow cooling rate (EDX01); second, a controlled oxidation in a thermogravimetric system (TGA02); and finally, an oxidation followed by a liquid nitrogen quenching (AES03). The

* Corresponding author. Tel.: +33 4 77 42 66 18; e-mail: wolski@emse.fr

Table 1. Experimental conditions of oxidation and type of analysis performed.

Sample	Oxidation conditions	Cooling	Analyses
EDX01	10 h, 950 °C, synthetic air with 20% O_2	Very slow cooling, ≈10 h, thermal inertia of furnace	SEM/EDX on the transverse cross-section
TGA02	100 h, 950 °C, He-20% O_2	Controlled cooling, 4 °C min^{-1}	TGA
AES03	10 h, 950 °C, synthetic air with 20% O_2	Quenching in liquid nitrogen, some seconds	AES coupled with Ar^+ ion sputtering and AES on the transverse polished section

sample EDX01 was analyzed by scanning electron microscopy (SEM) and EDX on its cross-section (Fig. 1a), oxidation kinetics was measured on the TGA02 sample by thermo-gravimetric analysis (TGA) and the AES03 sample was specifically prepared for two types of AES analyses (Fig. 1b and c).

SEM/EDX observations were performed using a JEOL JSM 6400 microscope equipped with a PGT analyser at 15 keV, with a 0.3 nA beam current. AES was performed with a Thermo VG Thetaprobe spectrometer using a field emission electron gun operating at 10 kV accelerating voltage, with a 5 nA beam current and a 45° tilt, resulting in a 150 nm effective spot size. Spectra were recorded on a hemispherical analyser in fixed retard ratio mode. Quantitative analysis by AES was performed measuring in direct spectra the ratio of te Auger peak height to its background close to the peak for the transitions Cr $L_3M_{2,3}V$ at 529 eV, Fe $L_3M_{2,3}M_{2,3}$ at 598 eV and Ni L_3VV at 848 eV. Analyses were carried out on the both AES03 sample and pure metal standards. Concentrations were calculated from intensities using the method described by Shimizu [11], which takes into account the variation in the backscattering coefficient and the mean free path of the Auger electrons as a function of composition [12]. Depth profiles were performed, using either combined steps of Ar^+ sputtering and AES analyses or AES spectra recorded directly on the cross-section of the sample. For the ion sputter depth profile, sputtering sequences were carried out using 3 keV argon ions onto a 1 mm^2 rastered area with a 19 μA cm^{-2} current density and an incidence angle of 45°. Under these conditions, the conversion of sputtering time scale into depth scale was done considering a constant sputtering rate of 1.65 nm min^{-1}, as experimentally measured on an Ni–5Cr model alloy and supposed to be three times lower in the oxide, i.e. during the first 1200 s of sputtering. It is worth noting that the AES signal comes from a depth of the order of 5 nm and that the sputtering procedure allows removal of the alloy by layers of approximately one nanometre close to the interface up to dozens or hundreds of nanometres far from the interface.

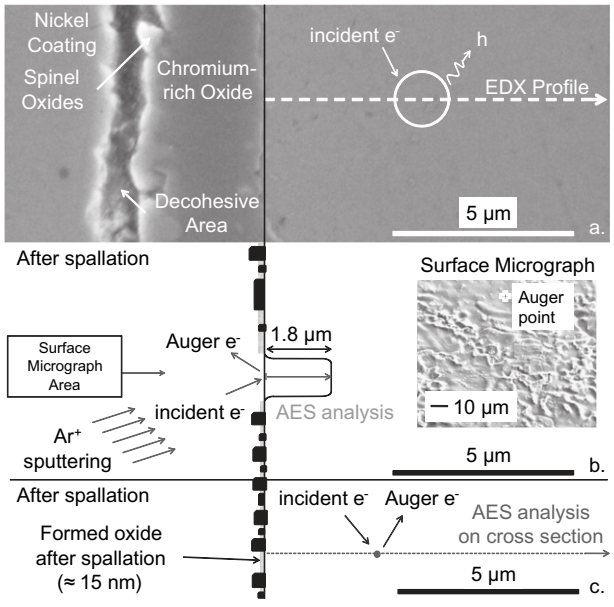

Figure 1. Description of the experimental analysis. (a) SEM/EDX analysis of the cross-section of EDX01. (b) Depth profiling by AES analysis coupled with ion sputtering of AES03 and the top view of the alloy surface after quenching showing the position of Auger point analysis. (c) AES analysis of the AES03 cross-section.

A complete chromium concentration profile was obtained by assembling an SEM/EDX profile in the area of its validity and an AES depth profile acquired from the oxide/alloy interface down to 2 μm from the oxide/alloy interface. The quality of the assembly procedure was validated by AES analysis of the cross-section, i.e. with 150 nm lateral resolution.

SEM/EDX concentration profiles were measured on an EDX01 specimen cross-section starting from the external oxide, through the chromium-depleted layer towards the bulk. The SEM micrograph (Fig. 1a) shows a representative cross-section of Ni–Cr–Fe alloy after a 10 h oxidation at 950 °C with a 3.5 μm thick chromium-rich oxide. The white arrow indicates the position where the EDX elemental Cr, Fe and Ni profiles were measured. The results of the EDX analyses (Fig. 2a) cover a distance that is longer than that represented by the white arrow in Figure 1a in order to reach the bulk chromium concentration. The chromium profile indicates strong chromium depletion down to a depth of approximately 15 μm, with an apparent minimum of 5 wt.% at a depth of 1.8 μm beneath the oxide/alloy interface. The presence of the chromium-rich oxide layer in fact induces an apparent increase in chromium content between 0 and 1.8 μm. The chromium detected in this part of the EDX profile comes from both the alloy and the oxide because of the size of the EDX interaction volume and interface irregularities.

In order to obtain a real Cr concentration profile on the first 2 μm close to the oxide/alloy interface, AES depth profiling was thought up. The main difficulty to be overcome is the presence of the thick oxide layer in the surface, which must be removed in order to use AES analysis coupled with ion sputtering (sputtering of this thick oxide would otherwise result in extremely high roughness, typically of the order of 1/10 of the

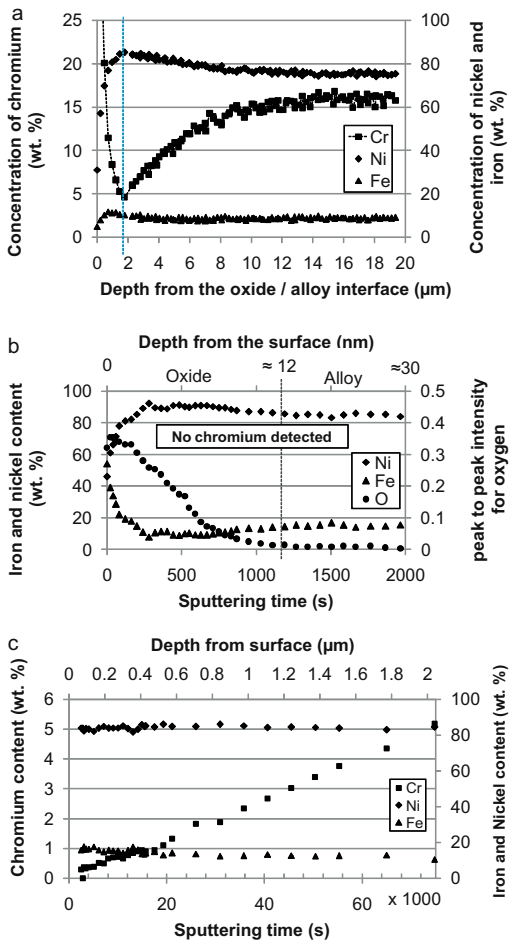

Figure 2. (a) Concentrations of chromium, iron and nickel by SEM/EDX as a function of distance from the oxide/alloy interface (sample EDX01). (b) AES depth profiles of analysis of the initial 30 nm of the AES03 sample (the "first step"), represented as weight concentrations for Fe and Ni, and as peak to peak divided by background ratios for oxygen, both as a function of sputtering time (chromium was not detected either in the oxide or immediately below the oxide). (c) AES depth profiles of the AES03 sample, starting from 30 nm down to 2 μm (the "second step"), as a function of sputtering time. Conversion to the depth scale was done based on a calibrated sputtering rate of 1.65 nm min^{-1} in the base alloy.

depth, i.e. approximately 350 nm). The possibility of removing the oxide layer and performing such an unusual AES analysis was demonstrated by careful TGA, which was initially performed to characterize the oxidation kinetics [2] and is briefly recalled below. This analysis was done on the TGA02 sample, which was oxidised at 950 °C for 100 h. The TGA results showed almost parabolic kinetics with an oxidation constant of 3.7×10^{-13} cm^2 s^{-1} (as defined by Wagner [1], i.e. the displacement between the initial position of metal and the actual oxide/alloy interface: $k_c = \Delta x^2_{metal}/2t$). The observation of major interest for the present work was that, during the cooling phase, a sudden drop in mass was detected on TGA curves at approximately 400 °C. The origin of this drop was interpreted as a spallation of the oxide layer. The spallation deduced from the TGA curves was confirmed for a shorter period of oxidation and enhanced by quenching in liquid nitrogen after 10 h of oxidation at 950 °C (AES03). The SEM micrograph included into Figure 1b shows that the spallation occurs at the oxide/alloy interface. Consequently, a depth profile analysis using AES combined with ion sputtering of this surface after quenching in liquid nitrogen allows the alloy composition in the first 2 μm to be obtained with the initial depth resolution in the nanometre range.

The AES depth profiles was obtained on the AES03 sample in two steps: (i) the first step (Fig. 2b), with an initial sputtering time of 2000 s, corresponding to a depth of approximately 30 nm, was performed with a standard detection limit of AES analyser, estimated to be 1 wt.%; (ii) the second step (Fig. 2c), with an additional sputtering time of 75,000 s, corresponding to a depth of slightly more than 2 μm, was performed with an optimised detection limit, estimated to be 0.2 wt.% of Cr. Both detection limits were measured using binary model alloys: Ni–0.2 wt.% Cr, Ni–1 wt.% Cr and Ni–5 wt.% Cr.

The first step profile (Fig. 2b) indicates the presence of a thin oxide film. This oxide film is assumed to form during quenching in liquid nitrogen, just after the spallation of a 3.5 μm thick oxide that occurs at around 400 °C, as deduced from the TGA curve. However, the most striking result is the absence of a chromium Auger peak, both in this thin oxide film and in the underlying alloy. It is clear from Figure 2b that a mixed Fe–Ni oxide was formed on the surface of the alloy during the cooling from 400 down to −196 °C in only a few seconds. This film was completely removed after 1200 s of sputtering. The remaining 800 s of sputtering removed a layer of approximately 20 nm. It is important to underline again that no chromium was detected either in the oxide or in the underlying alloy (with the standard detection limit of 1 wt.%).

The second step profile (Fig. 2c) started after a previous sequence of 2000 s, which completely removed the thin oxide layer together with approximately 20 nm of the alloy. The evolution of the chromium concentration in the chromium depleted underlayer, performed with a detection limit of 0.2 wt.%, indicates that the chromium content is clearly below 0.5 wt.% close to the oxide/alloy interface.

The results from Figure 2a and c enable the construction of a complete chromium depletion profile in the alloy. In fact, knowing the range of validity of the EDX profile and the sputtering rate during AES analysis enables these two profiles to be represented in the same figure (Fig. 3). Complementary AES analyses on the AES03 cross-section (cf. Fig. 1c), with a lateral resolution of 150 nm, were performed to validate this complete profile (grey circles in Fig. 3). This latter analysis confirms that the conversion from the sputtering time to the depth was correctly performed.

Consequently, AES measurements indicate a gradual decrease in the chromium content while approaching the oxide/alloy interface. The chromium concentration at the interface drops close to the detection limit. Under the conditions used in the present AES-based investigation, the chromium concentration at the interface does not exceed 0.5 wt.%.

Wagner's analytical solution for binary alloys [1] enables the chromium content at the oxide/alloy interface

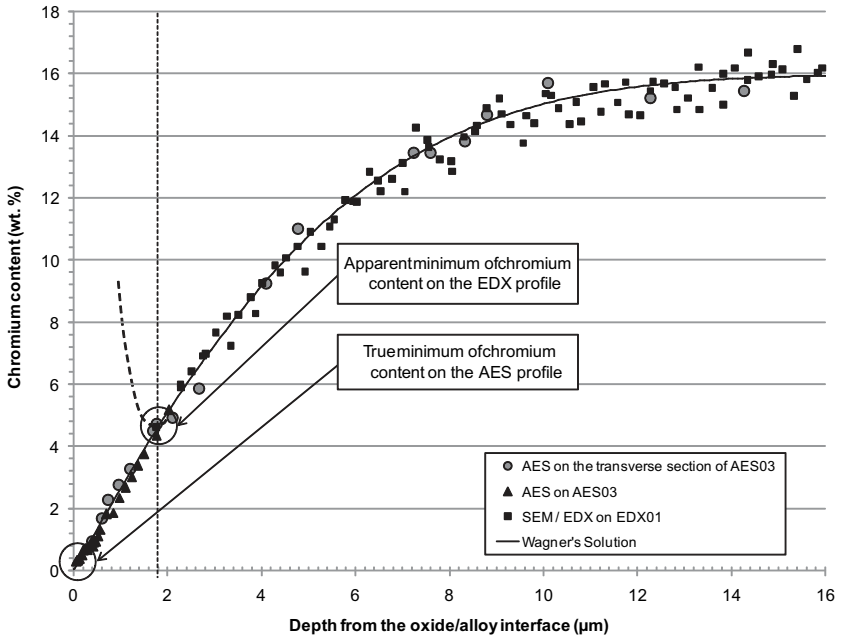

Figure 3. Complete chromium depletion profile obtained for an Ni–16Cr–9Fe alloy after 10 h of oxidation at 950 °C with 20% O_2. It shows a chromium content at the oxide/alloy interface of less than 0.5 wt.%. Black triangles correspond to AES measurements coupled with Ar^+ sputtering down to 2 µm depth with 5 nm initial depth resolution; black squares correspond to SEM/EDX measurements on the polished cross-section with 1.5 µm lateral resolution; and grey circles correspond to AES measurements on the polished cross-section with 150 nm lateral resolution. The continuous black line represents the best fit of Wagner's analytical solution obtained for a binary alloy.

to be calculated, providing the oxidation constant of pure chromium is known. Taking this value to be 4.2×10^{-13} cm^2 s^{-1} [4] and the chromium diffusion coefficient to be in the range 1.10^{-12}–2.10^{-11} cm^2 s^{-1} [13–16], the chromium content at the oxide/alloy interface has been calculated to be below 0.5 wt.%, even for the highest diffusion coefficient. Once the interface concentration is determined, Wagner's analytical approach [1] also gives the complete concentration profile of the oxidized element in the alloy. An estimation of the chromium diffusion coefficient was obtained from the best fit between Wagner's solution and the experimental profile, as shown in Figure 3, and resulted in a value of 5×10^{-12} cm^2 s^{-1}. This value corresponds to the average of the data reported in the literature [13–16].

It must be stressed that the results obtained in the present study concern a relatively short oxidation period of 10 h at 950 °C, where Wagner assumptions were satisfied. As far as we know, this is the first experimental demonstration of the validity of Wagner's solution for fcc alloys with such a low chromium interfacial concentration.

A complete chromium concentration profile was measured by AES and EDX on a high-purity Ni–16Cr–9Fe model alloy oxidized in air for 10 h at 950 °C. The chromium content in the immediate vicinity (i.e. within 20 nm) of the oxide/alloy interface is below 0.5 wt.%, as determined by AES with a detection limit of 0.2 wt.%. This value is confirmed by Wagner's analytical model for binary alloys, with the chromium diffusion coefficient determined to be 5×10^{-12} cm^2 s^{-1}.

We acknowledge M. Philippe Gilles from AREVA for financial support for this study.

[1] C. Wagner, J. Electrochem. Soc. 99 (10) (1952) 369.
[2] A. Nicolas, V. Barnier, N. Moulin, E. Aublant, E. Feulvarch, K. Wolski, Mat. & Tech. 99 (2011) 145–149.
[3] W.J. Quadakkers, Werkst. Kor. 36 (1985) 335–347.
[4] P. Moulin, A.M. Huntz, P. Lacombe, ActaMetall. 28 (1980) 745.
[5] C.S. Giggins, F.S. Pettit, Trans. Metall. Soc. AIME 245 (1969) 2495.
[6] G. Calvarin, R. Molins, A.M. Huntz, Oxid. Met. 53 (2000) 25.
[7] G.C. Woods, T. Hodgkiess, J. Electrochem. Soc, Volume 113 (4) (1966) 319.
[8] Y. Shida, G.C. Wood, F.H. Stott, D.P. Whittle, B.D. Bastow, Cor. Sci. 21 (1981) 581.
[9] P. Berthod, S. Michon, J. Di Martino, S. Mathieu, S. Noel, R. Podor, C. Rapin, Comput. Coupling Phase Diag. Thermochem. 27 (2003) 279.
[10] J. Killeen, A. Smith, R. Wild, Corros. Sci. 16 (1976) 551.
[11] R. Shimizu, Jpn. J. Applied Physics 22 (1983) 1631.
[12] S. Tanuma, C.J. Powell, D.R. Penn, Surface and Interface Analysis 21 (1993) 165.
[13] K. Monma, H. Suto, H. Oikawa, J. Jpn. Inst. Metals 28 (1964) 188.
[14] D.D. Pruthi, M.S. Anand, R.P. Agarwala, J. Nucl. Mater. 64 (1/2) (1977) 206.
[15] D. Delaunay, A.M. Huntz, P. Lacombe, Scr. Metall.Mater. 13 (6) (1979) 419.
[16] G.B. Fiedorow, E.A. Smirnow, F.I. Zomow, Miet. iMetallowied. czist. mietallow 4 (1963) 110.